

SYNTHESIS OF CuInSe₂(CIS) NANOSHEETS BY TWO LIQUID PHASE METHODS AND PHOTOELECTRIC PROPERTIES OF CIS THIN FILMS

X. L. CHEN^a, X. J. WANG^a, X. HUANG^b, Z. L. ZHAO^a, L. Z. BAI^a, W. J. LIANG^a, Y. L. MA^{a,*}

^aCollege of Physics and Electronic Information Engineering, Qinghai University for Nationalities, Xining 810007, China

^bKey Laboratory of Advanced Ceramics and Machining Technology of Ministry of Education, School of Materials Science and Engineering, Tianjin University, Tianjin 300072, China

Taking the all-green synthesis of copper indium selenium (CIS) material as the research purpose, we took Vitamin C (Vc) as a reducing agent and triethylene glycol (TEG) as a solvent to synthesize copper indium selenium(CIS) materials by solvothermal method and hot injection method, and discussed the advantages and disadvantages of the two synthetic methods. The dosage of Vc used in the two preparation methods was investigated, the process and mechanism of the chemical reaction were explained, and the thin film of the synthesized product was prepared and characterized. The experimental results showed that both liquid phase methods can be used to synthesize the single-phase chalcopyrite CIS nanosheets, and the performance of the product synthesized by the hot injection method was superior to that by the solvothermal method. The copper-poor structure Cu_{0.9}In_{0.94}Se₂ nanosheets with a band gap of 1.06 eV were synthesized by hot injection method. The carrier concentration and carrier mobility of the thin film prepared by the product synthesized by the hot injection method reached $1.08 \times 10^{16} \text{ cm}^{-3}$ and $120.62 \text{ cm}^2 \text{ V}^{-1} \text{ S}^{-1}$, respectively. The results showed that using Vc as a reducing agent, both liquid phase methods could be applied to produce single-phase chalcopyrite CIS nanosheets, which could achieve the universal use of Vc in liquid phase synthesis of CIS materials. Moreover, the products synthesized by hot injection method were more conducive to the preparation of high-performance thin films.

(Received April 24, 2020; Accepted August 4, 2020)

Keywords: Solvothermal method, Hot injection method, Reducing agent, Synthesis, CuInSe₂, Thin films, Photoelectric properties

1. Introduction

It is the main direction of current energy development to realize the sustainability of energy utilization. Promoting the efficient utilization of solar energy resources has the great significance for the realization of the sustainable development of energy and photoelectric

* Corresponding author: myl2005114@163.com

utilization is the main way to utilize solar energy resources. Among all kinds of solar cells[1-3], copper indium selenide-based thin film solar cells has become the first choice for the integrated development of future photovoltaic buildings due to their flexibility and low cost[4]. The current photoelectric conversion efficiency of such solar cells has exceeded 29%[5], which has potential research value.

The optical absorption layer is the core of copper indium selenide-based thin film solar cells[6], and its structural properties directly affects the efficiency of photoelectric conversion of the device[7]. To prepare CIS-based optical absorption layer with large particles and high compactness is of great significance for improving the performance of devices[8]. The structure and properties of CIS-based materials has significant influence on the preparation of thin films[9]. The main methods for preparing CIS-based materials include vacuum evaporation method[10, 11], sputtering method[12-15], liquid phase method[16-19], etc. CIS-based films with large particles can be directly prepared through vacuum methods such as vacuum evaporation and sputtering, etc, but their stoichiometry is uncontrollable and the cost is high. Liquid phase method has become the main method to synthesize CIS materials[20-23] due to its controllable stoichiometric ratio and simple doping process. However, when CIS-based materials are synthesized by liquid phase method, the main currently used reducing agents such as hydrazine hydrate[20], ethylenediamine[24], oleylamine[17, 25], etc[26]. are harmful, which are easy to cause environmental pollution during the preparation of the materials. It is a great challenge currently faced by liquid phase synthesis of CIS-based materials to avoid environmental pollution in the preparation process.

Here, we mainly aimed at the problem that the existing reducing agents are easy to pollute the environment in the preparation process of CIS materials. In order to realize the all-green synthesis of CIS materials, using Vc as reducing agent and TEG as solvent, the materials were synthesized by solvothermal method and hot injection method to investigate whether Vc could be universally used in liquid phase method synthesis of CIS materials.

2. Experimental

2.1. Chemicals

Copper(II) chloride (CuCl_2 97%), indium(III) chloride ($\text{InCl}_3 \cdot 4\text{H}_2\text{O}$, 99.9%), selenium powder (Se, 99.9%), polyvinylpyrrolidone (PVP, $M_w = 58,000$), absolute ethanol ($\text{C}_2\text{H}_5\text{OH}$, 99.99%), and triethylene glycol (TEG, 98%) were purchased from Aladdin and used as received without further processing.

2.2. Synthesis of CIS by solvothermal method

Firstly, 1mmol of $\text{CuCl}_2 \cdot 2\text{H}_2\text{O}$ and 1 mmol of $\text{InCl}_3 \cdot 4\text{H}_2\text{O}$ were weighed and dissolved in 5 mL TEG, and they were stirred at a rate of 600 r/min at 60 °C for 30 min until completely dissolved to obtain cationic precursor. Secondly, a certain amount of Vc, 0.10 g PVP and 25 mL TEG were added into the beaker, and they were stirred at a rate of 600 r/min at 60 °C for 30 min to prepare anionic precursor solution; after the anionic precursor solution was well prepared, the cationic precursor solution was injected into the anionic precursor solution, and they were stirred at a rate of 600 r/min below 80 °C for 30 min to fully mix the anionic and cationic precursor solution. Thirdly, the mixed

solution was added into a 50 ml polytetrafluoroethylene reactor and they were put into a muffle furnace. The temperature of the muffle furnace was increased to 300 °C at a heating rate of 10 °C/min and kept for 24 h, and then the temperature was reduced to 25 °C at a cooling rate of 10 °C/min, and then the reactor was taken out to obtain the target product. Finally, the obtained solution was washed 5 times in a centrifuge with absolute ethyl alcohol at the rotating speed of 9,000 r/min and the centrifugal time of 10 min and dried for later use.

2.3. Synthesis of CIS by thermal injection method

Firstly, 1 mmol of $\text{CuCl}_2 \cdot 2\text{H}_2\text{O}$ and 1 mmol of $\text{InCl}_3 \cdot 4\text{H}_2\text{O}$ were weighed and dissolved in 5 mL TEG, and they were stirred at a rate of 600 r/min at 60 °C for 30 min until completely dissolved to obtain cationic precursor. Secondly, a certain amount of Vc, 10 g PVP and 25 mL TEG were added into the three flasks, and they were stirred at room temperature for 10 min to prepare anionic precursor solution. Then three flasks were placed in a heating jacket, and connected to a thermal reaction reflux device, into which nitrogen was continuously introduced at a rate of 0.15 L/min after vacuuming and nitrogen introduction were operated alternately for 5 times, and the solution was heated to 260 °C while stirred at a rate of 600 r/min so that selenium powder was fully dissolved. Thirdly, the cationic precursor solution was rapidly injected into the anionic precursor solution at 260 °C, and the anionic precursor solution was refluxed at 250 °C for 1 h to obtain the target product. Finally, the obtained solution was washed 5 times in a centrifuge with absolute ethyl alcohol at the rotating speed of 9,000 r/min and the centrifugal time of 10 min and dried for later use.

2.4. Preparation of CIS thin films

First, the synthesized CIS was prepared into a spin-coating solution with a concentration of 0.05 g/ml in anhydrous ethanol and ultrasonically dispersed for 40 min at a frequency of 40 kHz, a temperature of 30 °C, and a power of 300 W. Then, the FTO conductive glass ($5 \times 5 \text{ cm}^2$) was ultrasonically cleaned with acetone and absolute ethanol and then dripped into the spin coating solution. It was accelerated to 150 rpm by a spin coater (MSC-400B, Mycro Technologies) at an acceleration rate of 10 r/min^2 for 3 min. Finally, the conductive glass was transferred to a hot plate (ZRX-27785, Beijing Zhongruixiang Technology Co., Ltd.) and baked at 30 °C for 5 min. The above process was repeated 3 times. After the films were prepared, the film and 0.2 g of selenium powder were added into a tubular furnace with a $6 \times 100 \text{ cm}^2$ quartz tube. The temperature was raised to 550 °C at a heating rate of 5 °C/min, and selenylation was carried out at this temperature for 30 min under Ar gas protection at a flow rate of 0.15 L/min.

2.5. Materials characterization

XRD patterns were obtained using an X-ray powder diffractometer (XRD, Bruker D8 Advanced, Germany) with $\text{Cu } K\alpha$ radiation at 40 kV and 40 mA. The microstructures and elemental composition of the products were characterized using scanning electron microscopy (SEM, JSM 7800F, Japan) and their respective energy-dispersive spectra. The UV-Vis-NIR spectra of CuInSe_2 thin films from 400 nm to 1500 nm were collected with a UV-Vis-NIR spectrophotometer (UV-3600, Shimadzu, Japan). Hall measurements were performed using a physical property measurement system (PPMS, Quantum Design PPMS-9, America).

3. Result and discussion

3.1. Effect of Vc dosage on product synthesis

Fig. 1 shows the XRD patterns of the products synthesized by the two methods at different Vc dosage. As can be seen from Fig. 1 (a), when the dosage of Vc was 0.10 g, the diffraction pattern contained strong diffraction peaks at $2\theta = 26.57^\circ$, 44.23° and 52.39° , which are consistent with the main characteristic diffraction peaks of chalcopyrite-phase CuInSe_2 (JCPDS:40-1487) on (112), (220) and (312) crystal planes. There are four weak diffraction peaks at $2\theta = 28.11^\circ$, 31.10° , 46.05° and 50.01° were consistent with the main characteristic diffraction peaks of CuSe (JCPDS:34-1071) on (102), (006), (110) and (108) crystal planes. Therefore, when the dosage of Vc was 0.10 g, the main phase composition in the synthesized product was chalcopyrite-phase CuInSe_2 (JCPDS:40-1487). There was also one impurity phases of CuSe (JCPDS: 34-1071). When the dosage of Vc was increased to 0.20 g, the phase composition of the product was basically CuInSe_2 , but there was a very weak characteristic diffraction peak of CuSe on (112) crystal planes at $2\theta = 28.11^\circ$. When the dosage of Vc was increased to 0.25 g, the characteristic diffraction peaks of CuSe disappeared completely, and the weak diffraction peaks appeared at $2\theta = 27.68^\circ$, 30.87° , 41.91° , mainly on (103), (200), (105/213) crystal planes of CIS, indicating that a single-phase chalcopyrite CuInSe_2 with good crystallinity was prepared. In Fig.1 (b), when the dosage of Vc was 0.1 g, the main phase component of the products was chalcopyrite-phase CuInSe_2 , with a small amount of CuSe impurity phase. When the dosage of Vc as 0.15 g, the characteristic diffraction peak of CuSe was weakened. When the dosage of Vc was 0.20 g, the diffraction of the characteristic diffraction peak of CuSe completely disappeared, and a single-phase CuInSe_2 was synthesized. When the dosage of Vc was increased to 0.25 g again, the diffraction peak intensity and peak width of the product had no obvious difference compared with that of 0.20 g Vc, indicating that when the dosage of Vc exceeded 0.20 g, the dosage of Vc had little effect on the phase composition and crystallinity of the product.

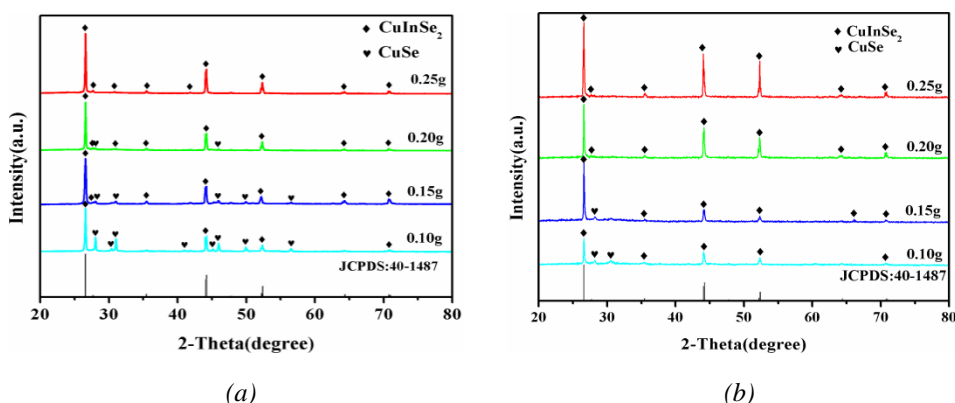


Fig. 1. XRD patterns of synthesized products by (a) solvothermal method and (b) hot injection method at different Vc dosages.

According to the above analysis, it could be concluded that in the process of synthesizing 1

mmol of CIS material, the demand for Vc dosage by solvothermal method should be no less than 0.25 g, while that by hot injection method no less than 0.20 g. Then increasing Vc dosage again on this basis would not have great influence on the phase composition and crystallinity of the product. The reason why the demand for Vc dosage in solvothermal method was greater than that in hot injection method, it may be that the solution in solvothermal method was static during the reaction process, which cannot make the reducing agent effectively act on the whole reaction space, resulting in insufficient local reaction, and thus increasing the demand for reducing agent dosage.

3.2. Characterization of CIS nanosheets

According to the discussion in 3.1, CIS was synthesized through two methods with the best Vc dosage respectively (the samples synthesized by solvothermal method and hot injection method were called sample 1 and sample 2 respectively), and the phase structure and composition of the synthesized products were characterized as shown in Figs. 2, 3 and 4.

Figs. 2 (a) and (b) are XRD original and partial enlarged patterns of sample 1 and sample 2, respectively. As can be seen from Fig. 2 (a), the phase composition of the two samples was the single-phase chalcopyrite CIS with good crystallinity without other impurity phase. To further understand the crystallinity of the samples, the main characteristic diffraction peaks of the two samples at $2\theta=26.57^\circ$ were enlarged as shown in Fig. 2 (b). The half-peak width of characteristic diffraction peak of sample 1 was narrower. This indicated that CIS synthesized by solvothermal method had better crystallinity. But the crystallinity of the two samples was not significantly different although sample 2 was slightly worse than sample 1 in half-peak width.

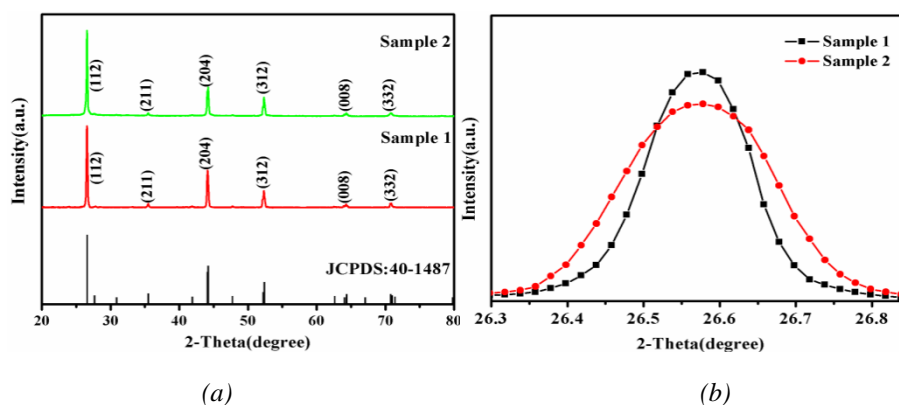
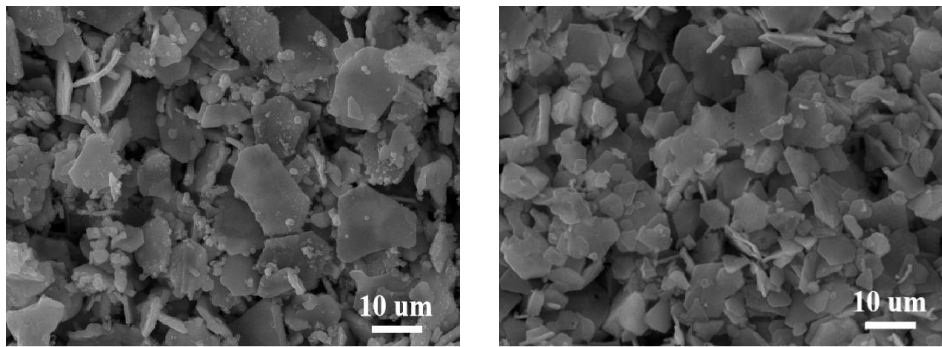


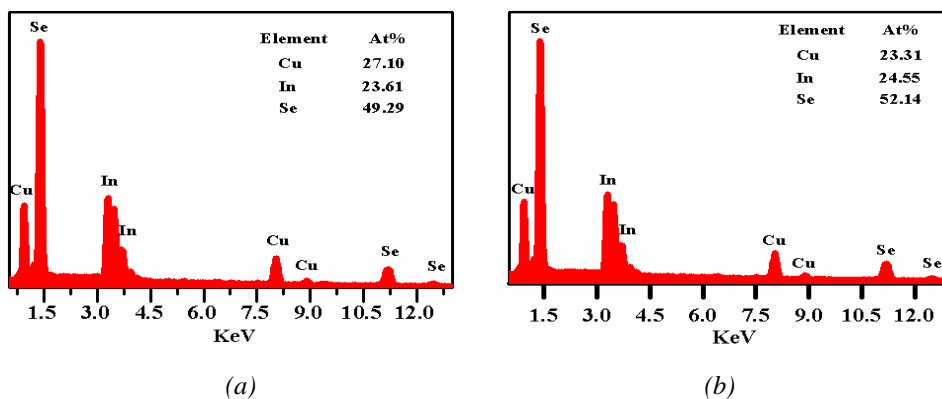
Fig. 2. XRD patterns of sample 1 and sample 2: (a) Original pattern, (b) Partial enlarged pattern.

Figs. 3 (a) and (b) are SEM images of sample 1 and sample 2, respectively. It can be seen that the particle morphology of sample 1 and sample 2 were both nanosheets. For sample 1, there were larger particles with the particle size of up to more than 20 μm , and it also has a large number of fine particles with the particle size of basically about several microns, resulting in a smaller average particle size of about 10 μm , and poor uniformity of particle size distribution. For sample 2, there were no extremely large or small particles in its particle size distribution with the average particle size of up to about 13 μm . So sample 2 was better than the uniformity of particle size distribution of sample 1.



(a) (b)
Fig. 3. SEM images of (a) sample 1 and (b) sample 2.

The EDS elemental maps were used to measure the atomic content of the sample 1 and sample 2, the results are shown in Fig. 4. The molar ratios of Cu, In and Se in sample 1 were 27.10%, 23.61% and 49.29%, respectively, which corresponded to a chemical formula of $\text{CuIn}_{0.87}\text{Se}_{1.82}$, it basically consistent to the proportion of atomic ratio of 1:1:2 in CIS chemical formula but formed CIS with copper-rich structure. The molar ratios of Cu, In and Se in sample 2 were 23.31%, 24.55% and 52.14% respectively, which corresponded to a chemical formula of $\text{Cu}_{0.9}\text{In}_{0.94}\text{Se}_2$, it closer to the theoretical ratio of the three atoms in CIS chemical formula and formed CIS with copper-poor structure. Although the copper-poor property was not as good as the copper-rich property in promoting grain growth and film compactness, it was beneficial to inhibit the generation of Cu_{2-x}Se in the phase[7]. The presence of Cu_{2-x}Se in the absorption layer of photoelectric devices would reduce the separation of photoelectric carriers, which would lead to the degradation of the interface performance of the absorption layer[4]. Therefore, the copper-poor structure can effectively promote the separation of photo-generated carriers and has a positive effect on improving the voltage of the devices.



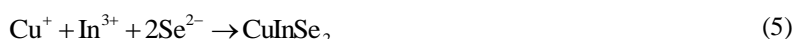
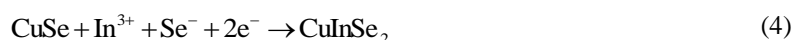
(a) (b)
Fig. 4. Energy-dispersive X-ray spectra of (a) sample 1 and (b) sample 2.

Discuss the advantages and disadvantages of the two synthetic methods by comparing the properties of the two samples. According to the above analysis, although the crystallinity of CIS nanosheets, synthesized by hot injection method was not as good as that of solvothermal method,

but their particle size distribution was more uniform, the average particle size was larger, and CIS with copper-poor structure was formed. The reasons for this difference may be that in the process of solvothermal synthesis of products, longer reaction time and higher reaction temperature were more conducive to Oswald ripening[27] and could promote crystallinity, but the chemical reaction occurred gradually with the increase of temperature and the advancement of time, so the crystal gradually nucleated and grew up in the early stage of the reaction to produce larger particles, and smaller particles would be produced in the late stage of the reaction due to the lack of growth power, resulting in not uniform particle size distribution of nanosheets. The synthesis of CIS by hot injection method involved cation injection at a specific temperature, instantaneous and intense chemical reactions would be formed with a large number of explosive nucleation, which was conducive to improving the uniformity of particles but not conducive to the growth of crystals. However, due to the low reaction temperature and short reflux time, the crystals did not have enough temperature and time to carry out Oswald ripening[27], so that the crystallinity of the crystals was poor.

3.3. Process and mechanism of chemical reaction

Vitamin C has 4 -OH groups in its molecular formula, which showed strong reducing in TEG at high temperatures, so that selenium powder was reduced and participated in the chemical reaction. The specific chemical reactions are as follows:



Vc and TEG showed strong chemical reducibility under the action of high temperature, causing Se powder to undergo chemical reaction (1), producing Se^{2-} and Se^- . Similarly, due to the strong chemical reduction power promote Cu^{2+} to be reduced to Cu^+ , resulting in the occurrence of chemical reaction (2). Because the chemical bond of In-Se is stronger than that of Cu-Se[28], under the condition of the coexistence of In^{3+} , Cu^{2+} and Se^{2-} , CuSe was formed firstly[7] and chemical reaction (3) occurs. Then CuSe reacted with In^{3+} and Se^- as shown in reaction (4), generating CIS and undergoing phase transition from CuSe to CuInSe_2 . At the same time, there were also chemical reactions (1), (2) and (5), which directly generated CIS without phase transition from CuSe to CuInSe_2 . However, when the Vc content is too low, the overall chemical reduction ability will be weak, which is insufficient to provide enough reduction power for Cu^{2+} , so that there is a large amount of Cu^{2+} in the reaction solution. As a result, the chemical reactions of (4) was insufficient, and there was impurity phase CuSe in the target products, which also explained the phenomenon in 3.1 that CuSe would exist in the product when the dosage of Vc was too low.

3.4. Surface structure and photoelectric properties of thin films

Sample 1 and Sample 2 were prepared as thin films (the thin films prepared by Sample 1 and Sample 2 were called thin film 1 and thin film 2 respectively) and characterized. Fig. 5(a) and (b) show the surface SEM images of thin film 1 and thin film 2 respectively. It could be seen that there were more raised film boundaries in film 1, resulting in a large number of film defects, and the formed film surface was rougher. Compared with film 1, film 2 had fewer raised film boundaries on the surface, and the continuity of the film was better, forming a relatively dense CIS film. From the enlarged view of the part of the film, the size of the particles forming the film increased compared with that before the film was prepared, and the thickness of the nanosheet also increased. This might be caused by selenylation, which was conducive to promoting ion diffusion and crystal growth[8].

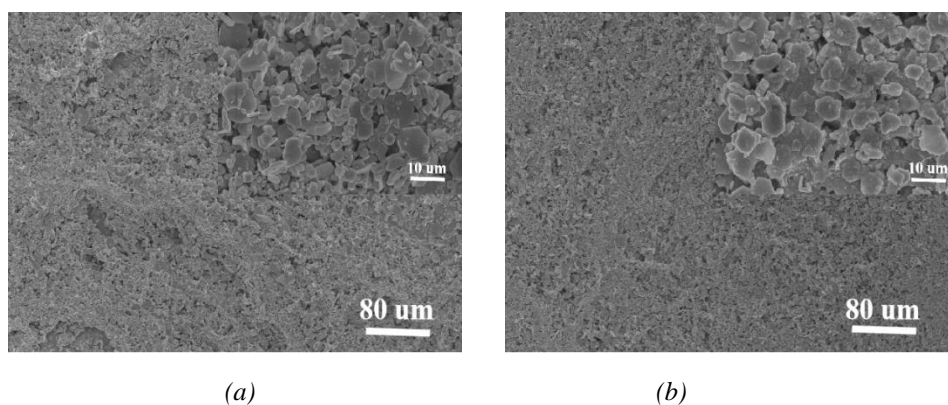


Fig. 5. Surface SEM images of (a) thin film 1 and (b) thin film 2.

The light absorption characteristics of the thin film were tested by a UV-vis-NIR spectrophotometer, and the band gap of the material was deduced according to Tauc's formula as shown in Fig. 6. It could be seen that the absorption value of both films increased slowly from 1,200 - 900 nm, and increased sharply from 900 - 400 nm, which shows good absorption in both visible and near-infrared regions. They conformed to the optical absorption characteristics of CIS films, but the absorption of film 2 in visible region was slightly better than that of film 1. As can be seen from Fig. 6 (b), the band gap of thin film 1 material and thin film 2 material were 1.08 eV and 1.06 eV respectively. In comparison, the band gap of thin film 2 material was closer to the theoretical value of 1.04 eV[29], but the values of both thin film materials were greater than the theoretical value, which might be caused by internal defects of the materials. This also showed that the internal defects of the film 2 material were less than those of the film 1.

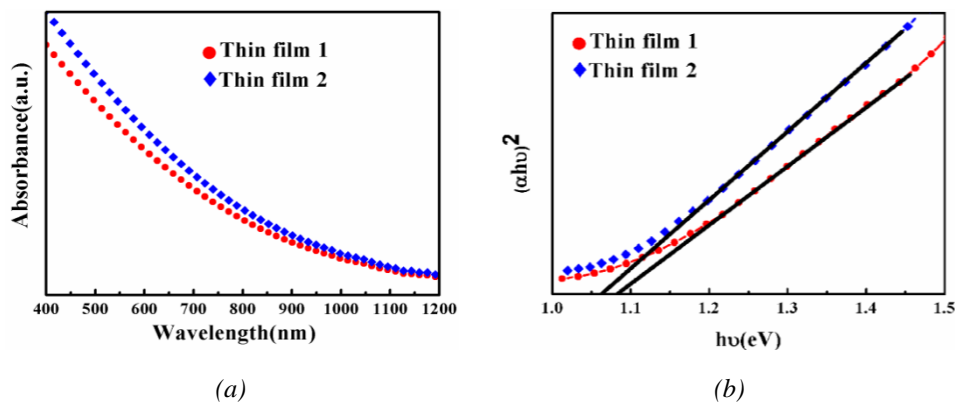


Fig. 6. (a) UV-vis-NIR absorbance spectra and (b) Tauc plot of two thin films.

Table 1 shows the electrical performance parameters of the thin films. It can be seen that both the thin film 1 and the thin film 2 display characteristics of the P-type semiconductors. The electrical resistivity, carrier concentration and carrier mobility of film 1 were 52.4 $\Omega\cdot\text{cm}$, $8.47 \times 10^{15} \text{ cm}^{-3}$ and $90.43 \text{ cm}^2 \text{ V}^{-1} \text{ S}^{-1}$, respectively and those of film 2 were 34.79 $\Omega\cdot\text{cm}$, $1.08 \times 10^{16} \text{ cm}^{-3}$ and $120.62 \text{ cm}^2 \text{ V}^{-1} \text{ S}^{-1}$, respectively. Comparatively, the electrical resistivity of the thin film 2 was lower, its carrier concentration and carrier mobility were higher. More importantly, the carrier concentration of the thin film 2 reached 10^{16} , which met the requirements for preparing the photosensitive layer of high-performance photoelectric devices[25].

Table 1. Electrical performance parameters of two thin films.

Film name	Conductivity	Electrical resistivity/ $\Omega\cdot\text{cm}$	Carrier concentration/ cm^{-3}	Carrier mobility/ $\text{cm}^2 \text{ V}^{-1} \text{ S}^{-1}$
Thin film 1	p	52.24	8.47×10^{15}	90.43
Thin film 2	p	34.79	1.08×10^{16}	120.62

According to the above analysis, compared with film 1, film 2 had higher surface compactness, fewer defects, the band gap of the material was closer to the theoretical value, and its three main electrical performance parameters were also better than those of film 1. This showed that the CIS material synthesized by hot injection method was more suitable for the preparation of thin films. The reasons for the above differences may be as follows: Firstly, the CIS material synthesized by hot injection method had a larger average particle size and a more uniform particle size distribution, which was more conducive to the formation of a film with uniform interior and smooth surface during the film preparation process, and can effectively avoid the generation of internal defects of the film[8]. Secondly, the band gap of CIS material synthesized by hot injection method was closer to the theoretical value, which proved that the material had fewer internal defects. More importantly, the material formed a copper-poor structure. For chalcopyrite CIS, fewer internal defects of the material and the properties of copper-poor structure were more conducive to promoting the separation and migration of photo-generated carriers[30, 31]. The 2 reasons might lead to the photoelectric properties of the thin film 2 being better than those of the thin film 1.

4. Conclusions

1) Using Vc as a reducing agent, single-phase chalcopyrite CIS nanosheets can both be synthesized by solvothermal method and hot injection method. However, In the process of synthesizing 1 mmol of CIS material, the demand for Vc dosage by solvothermal method should be no less than 0.25 g, while that by hot injection method no less than 0.20 g.

2) Compared with solvothermal method, the CIS nanosheets synthesized by hot injection method had fewer defects and more uniform particle size distribution. CIS nanosheets with copper-poor structure with a band gap of 1.06 eV and chemical formula of $\text{Cu}_{0.9}\text{In}_{0.94}\text{Se}_2$ were synthesized, whose average particle size and thickness were about 15 μm and 0.9 μm respectively. CIS nanosheets synthesized by hot injection method were more conducive to the preparation of CIS thin films with high performance. The carrier concentration and carrier mobility of the thin films reached $1.08 \times 10^{16} \text{ cm}^{-3}$ and $120.62 \text{ cm}^2 \text{ V}^{-1} \text{ S}^{-1}$, respectively.

3) The phase transition from CuSe to CuInSe_2 was observed in the chemical reaction of synthesizing CIS materials in this experiment. When the dosage of reducing agent could not meet the minimum requirement of chemical reaction, the product would have impurity phase due to insufficient phase transition.

Based on the above conclusions, using Vc as the reducing agent and triethylene glycol as the solvent, the solvothermal method and the hot injection method can not only be utilized to prepare single-phase chalcopyrite CIS materials, but effectively avoid the environmental pollution caused by the existing reducing agents during preparation, reaching the purpose that Vc can be commonly used in the liquid phase synthesis of CIS materials.

Acknowledgements

The authors acknowledge the financial support from Key Natural Science Foundation of Qinghai province (2017-zj-729).

References

- [1] L. Zhang, H. Rao, Z. Pan, X. Zhong, *ACS Appl. Mater. Interfaces* **11**(44), 41415 (2019).
- [2] H. Guthrey, A. Norman, J. Nishinaga, S. Niki, M. Al-Jassim, H. Shibata, *ACS Appl. Mater. Interfaces* **12**(2), 3150 (2019).
- [3] E. Akman, S. Akin, T. Ozturk, B. Gulveren, S. Sonmezoglua, *Sol. Energy* **202**, 227 (2020).
- [4] D. B. Mitzi, M. Yuan, W. Liu, A. J. Kellock, S. J. Chey, V. Deline, A. G. Schrott, *Adv.Mater.* **20**(19), 3657 (2008).
- [5] T. Kato, J. Wu, Y. Hirai, H. Sugimoto, V. Bermudez, *IEEE J. Photovolt.* **9**(1), 325 (2019).
- [6] C. H. Chung, S. H. Li, B. Lei, W. Yang, W. W. Hou, B. Bob, Y. Yang, *Chem. Mater.* **23**(4), 964 (2011).
- [7] M. Turcu, O. Pakma, U. Rau, *Appl. Phys. Lett.* **80**(14), 2598 (2002).
- [8] K. L. Chopra, P. D. Paulson, V. Dutta, *Prog. Photovolt: Res. Appl.* **12**(23), 69 (2004).
- [9] I. M. Kötschau, H. W. Schock, *J. Phys. Chem. Solids* **64**(10), 1559 (2003).
- [10] S. J. Ahn, C. W. Kim, J. H. Yun, J. Gwak, S. Jeong, B. H. Ryu, K. H. Yoon, *J. Phys.Chem. C* **114**, 8108 (2010).
- [11] B. Maheswari, M. Dhanam, *J Mater Sci: Mater Electron* **24**(9), 3481 (2013).
- [12] X. Huang, X. L. Chen, Z. W. Zhang, H. M. Ji, Y. L. Ma. *Chalcogenide Letters* **16**(11), 545(2019).
- [13] P. Liu, Z. Liu, C. Qin, T. He, B. Li, L. Ma, K. Shaheen, J. Yang, H. Yang, H. Liu, K. Liu, M. Yuan, *Sol. Energy Mater. Sol. Cells* **212**, 110555 (2020).
- [14] J. Li, H. Shen, J. Chen, Y. Li, J. Yang, *Phys. Chem. Chem. Phys.* **18**(41), 28829 (2016).
- [15] T. P. Dhakal, C. Y. Peng, R. R. Tobias, R. Dasharathy, C. R. Westgate, *Sol. Energy* **100**, 23 (2014).
- [16] M. He, D. Kou, W. Zhou, Z. Zhou, Y. Meng, S. Wu, *Inorg. Chem.* **58**(19), 13285 (2019).
- [17] D. W. Houck, S. V. Nandu, T. D. Siegler, B. A. Korgel, *ACS Appl. Nano Mater.* **2**(7), 4673 (2019).
- [18] P. Jiang, P. Boulet, M. C. Record, *J. Mater. Chem. C* **7** (19), 5803 (2019).
- [19] T. Kodalle, D. Greiner, V. Brackmann, K. Prietzel, A. Scheu, T. Bertram, P. Reyes-Figueroa, T. Unold, D. Abou-Ras, R. Schlatmann, C. A. Kaufmann, V. Hoffmann, *J. Anal. At.Spectrom* **34**(6), 1233 (2019).
- [20] H. Liu, Z. Jin, W. Wang, J. Li, *CrystEngComm.* **13**(24), 7198 (2011).
- [21] D. W. Houck, E. I. Assaf, H. Shin, R. M. Greene, D. R. Pernik, B. A. Korgel, *J. Phys. Chem. C* **123**(14), 9544 (2019).
- [22] N. Oh, L. P. Keating, G. A. Drake, M. Shim, *Chem. Mater.* **31**(6), 1973 (2019).
- [23] T. Yan, Y. Li, X. Song, J. Wang, Z. Xie, D. Deng, *J. Mater. Chem. C* **7**(24), 7279 (2019).
- [24] M. Ye, R. Tang, S. Ma, Q. Tao, X. Wang, Y. Li, P. Zhu, *J. Phys. Chem. C* **123**(34), 20757 (2019).
- [25] R. Noufi, R. Axton, C. Herrington, S. K. Deb, *Appl. Phys. Lett.* **45**(6), 668 (1984).
- [26] G. Jia, K. Wang, B. Liu, P. Yang, J. Liu, W. Zhang, R. Li, C. Wang, S. Zhang, J. Du, *RSC Adv.* **9**(61), 35780 (2019).
- [27] P. W. Voorhees, *J. Stat. Phys.* **38**, 231 (1985).

- [28] J. Xu, C. S. Lee, S. T. Lee, Y. B. Tang, W. X. Zhang, X. Chen, Z. Yang, *ACS Nano* **4**(4), 1845 (2010).
- [29] T. J. Whang, M. T. Hsieh, Y. C. Kao, S. J. Lee, *Appl. Surf. Sci.* **255**(8), 4600 (2009).
- [30] S. Jung, S. Ahn, J. H. Yun, J. Gwak, D. Kim, K. Yoon, *Curr. Appl. Phys.* **10**(4), 990 (2010).
- [31] O. Lundberg, M. Bodegård, J. Malmström, L. Stolt, *Prog. Photovolt: Res. Appl.* **11**(2), 77 (2003).